Monoclonal Antibodies to Human Lymphocyte Homing Receptors Define a Novel Class of Adhesion Molecules on Diverse Cell Types

Louis J. Picker,*§ Maurice Nakache,*‡§ and Eugene C. Butcher*§

*Laboratory of Experimental Oncology, Department of Pathology, Stanford University School of Medicine and ‡Stauffer Laboratory for Physical Chemistry, Department of Chemistry, Stanford University, Stanford, California 94305; and §Palo Alto Veterans Administration Medical Center, Palo Alto, California 94304

Abstract. A 90-kD lymphocyte surface glycoprotein, defined by monoclonal antibodies of the Hermes series, is involved in lymphocyte recognition of high endothelial venules (HEV). Lymphocyte gp90^{Hermes} binds in a saturable, reversible fashion to the mucosal vascular addressin (MAd), a tissue-specific endothelial cell adhesion molecule for lymphocytes. We and others have recently shown that the Hermes antigen is identical to or includes CD44 (In[Lu]-related p80), human Pgp-1, and extracellular matrix receptor III—molecules reportedly expressed on diverse cell types. Here, we examine the relationship between lymphoid and non-lymphoid Hermes antigens using serologic, biochemical, and, most importantly, functional assays. Consistent with studies using mAbs to CD44 or Pgp-1, mAbs against five different epitopes on lymphocyte gp90^{Hermes} reacted with a wide variety of nonhematolymphoid cells in diverse normal human tissues, including many types of epithelium, mesenchymal elements such as fibroblasts and smooth muscle, and a subset of glia in the central nervous system. To ask whether these non-lymphoid molecules might also be functionally homol-ogous to lymphocyte homing receptors, we assessed their ability to interact with purified MAd using fluorescence energy transfer techniques. The Hermes antigen isolated from both glial cells and fibroblasts—which express a predominant 90-kD form similar in relative molecular mass, isoelectric point, and protease sensitivity to lymphocyte gp90^{Hermes}—was able to bind purified MAd. In contrast, a 140–160-kD form of the Hermes antigen isolated from squamous epithelial cells lacked this capability. Like lymphocyte binding to mucosal HEV, the interaction between glial gp90^{Hermes} and MAd is inhibited by mAb Hermes-3, but not Hermes-1, suggesting that similar molecular domains are involved in the two binding events. The observation that the Hermes/CD44 molecules derived from several nonlymphoid cell types display binding domains homologous to those of lymphocyte homing receptors suggests that these glycoproteins represent a novel type of cell adhesion/recognition molecule (H-CAM) potentially mediating cell-cell or cell-matrix interactions in multiple tissues.

S PECIFIC cell–cell and cell–matrix adhesion is a fundamental property of multicellular organisms, accounting, at least in part, for the development and maintenance of specialized cellular form and function (for reviews see Edelman and Thiery, 1985; Jessell, 1988; Obrink, 1986). Although a vast array of specific cellular recognition/adhesion events must occur during ontogeny, recent studies have revealed evolutionary mechanisms that would tend to reduce the total number of genes and polypeptides needed to mediate these interactions. Foremost among these mechanisms is the phenomenon that individual or closely related families of cell adhesion molecules (CAMs)[1] are expressed in a variety of different tissues and probably participate in diverse cellular interactions at these distinct anatomic sites. For ex-ample, the neural cell adhesion molecule (N-CAM), the cadherins, the integrins, and intercellular adhesion molecule-1 (ICAM-1) are all expressed by multiple and varied cell types of distinct histogenetic origin (Crossin et al., 1985; Hatta et al., 1987; Ruoslahti et al., 1985; Dustin et al., 1986). It follows from these examples that molecules with demonstrated cell recognition/adhesion activity in one setting are potential candidates for homologous function in different settings.

Our laboratory has previously characterized a class of 90-kD human lymphocyte cell surface glycoproteins (defined by antibodies of the Hermes series) that is involved in the heterotypic recognition of high endothelial venules (HEV), the specialized venules in lymphoid organs and sites of chronic inflammation that mediate lymphocyte extravasation in the process of lymphocyte homing (for reviews see Jalkanen et al., 1986a; Berg et al., 1989). In general, lymphoid populations lacking these glycoprotein "homing receptors" are unable to effectively interact with HEV, and antibodies to

---

1. *Abbreviations used in this paper:* CAM, cell adhesion molecule; F-MAd, FITC-conjugated mucosal vascular addressin; HEV, high endothelial venules; HFF, human foreskin fibroblasts; MAd, mucosal vascular addressin; TR, Texas red; TL, tonsil lymphocytes.

specific epitopes on gp90^Hermes inhibit tissue-specific HEV binding (Jalkanen et al., 1986b, 1987). One ligand for lymphocyte homing receptors, a 58–66-kD protein expressed by HEV in mucosal lymphoid tissue (mucosal vascular addressin [MAd]), has been identified (Streeter et al., 1988a; Nakache et al., 1988), and specific, saturable binding of purified gp90^Hermes to purified MAd has been demonstrated with fluorescence energy transfer techniques (Nakache, M., E. L. Berg, L. J. Picker, and E. C. Butcher, manuscript submitted for publication).

We and others have recently demonstrated that the Hermes class of lymphocyte homing receptors are the same as, or include, the CD44 (In[Lu]-related p80) and human Pgp-1 antigens (Picker et al., 1989) and the extracellular matrix receptor III (Gallatin, W. M., E. Wayner, T. St. John, E. C. Butcher, and W. Carter, manuscript submitted for publication), molecules which have been reported to be expressed on a variety of nonhematolymphoid cell types (Letarte et al., 1985; Quackenbush et al., 1985, 1986; Daar and Fabre, 1981, 1983; McKenzie et al., 1982; Isacke et al., 1986; Carter and Wayner, 1988). Here, using mAbs recognizing five distinct epitopes on lymphocyte gp90^Hermes, we confirm the widespread expression of molecules closely related to these lymphocyte homing receptors. Most importantly, we demonstrate that some of these nonlymphoid antigens possess ligand-binding sites homologous to those of lymphocyte homing receptors. These findings suggest that this class of glycoproteins has broad functional significance, perhaps serving as CAMs in diverse settings.

Materials and Methods

Tissue and Cells

Samples of snap-frozen normal human tissues for immunostaining were obtained from the Department of Pathology's frozen tissue bank at Stanford University (Stanford, CA). Tonsil lymphocytes (TL) were obtained by gentle mincing and washing of fresh human tonsil specimens over type 304 steel screen (Tylinter, Mentor, OH) in RPMI-1640 media. The collected TL were washed twice by centrifugation through RPMI-1640 media before preparation of lysates (see below). The human glioma cell line HS683 (HTB138) was obtained from the American Type Culture Collection (Rockville, MD). Human foreskin fibroblasts (HFF) were a kind gift of Dr. M. Bernfield (Stanford University, Stanford, CA), and were used as passage 6–8. Characteristics of the human keratinocyte cell line SCL-1 (derived from a human squamous cell carcinoma of the skin) and the human lymphoid cell line KCA have been described previously (Boukamp et al., 1982; Jalkanen et al., 1986b, 1987).

Antibodies and Immunostaining

The isolation and characterization of mAbs of the Hermes series—Hermes-1 (rat IgG2a), Hermes-2 (rat IgG2a), Hermes-3 (mouse IgG2a), H2-7 (mouse IgG1), and H3-51 (mouse IgG2b)—have been described previously (Jalkanen et al., 1986b, 1987; Picker et al., 1989). All of these mAbs recognize identical bands on Western blots of lymphoid cell lysates, and these bands are all entirely precleared with the Hermes-1 mAb. Cross-blocking studies indicate that mAbs Hermes-1, -2, and -3 define sterically independent epitopes. H2-7 and H3-51 are cross-blocked by Hermes-2 and -3, respectively, but have been determined to see different epitopes by other criteria (Goldstein et al., 1989). For example, Hermes-3, but not H3-51, recognizes Hermes antigen homologues on monkey, goat, and sheep lymphocytes. Furthermore, both H2-7 and H3-51 react with the fusion proteins from the recently isolated Hermes-specific cDNA clones λ3A21 and λ14-1 (λgt11 expression system). Hermes-3 reacts only with the λ3A21 fusion protein, whereas Hermes-2 is nonreactive with both. The reactivity of H2-7, H3-51, and Hermes-3 with fusion proteins produced in a bacterial expression system indicate that the epitopes recognized by these antibodies are not depen-

dent on normal human posttranslational processing. All antibodies were used under saturating conditions. Species- and isotype-matched mAbs of irrelevant specificity were used as controls.

Examination of the distribution of Hermes antigen in various tissues was done on acetone-fixed cryostat sections using both indirect immunofluorescence (Haynes et al., 1982), and a three-stage biotin-avidin immunoperoxidase technique (Bindl and Warnke, 1986). For some tissues (i.e., those with high backgrounds using the biotin-avidin system), these techniques were supplemented with a two-stage immunoperoxidase procedure, as previously described (Streeter et al., 1988a,b). For immunostaining of adherent tissue culture cells, cells were grown on tissue culture chamber slides (Miles Laboratories Inc., Naperville, IL) and stained unfixed by indirect immunofluorescence.

Antigen Preparation and Quantitation

Lysates were prepared by incubating cells in lysis buffer (2% NP-40, 150 mM NaCl, 1 mM MgCl$_2$, 10 μg/ml Aprotinin, and 1 mM PMSF in 20 mM Tris-HCl, pH 7.5) for 30 min at room temperature. TL and KCA were lysed at 4×10^7 cells/ml. The adherent cell lines were lysed directly in the culture flasks (cultures at 80–90% confluence) after extensive rinsing with RPMI-1640 media using 5 ml lysis buffer per flask (Falcon T-175; Becton Dickinson Labware, Lincoln Park, NJ). Lysates were clarified by centrifugation (48,000 g for 30 min at 4°C) followed by passage through 0.2-μm filters (Nalge Co., Rochester, NY). Hermes antigens were isolated by passage of the crude lysates over a precolumn of normal rat IgG (Cappel Laboratories, West Chester, PA) coupled to Sepharose 4B followed by a Hermes-1-Sepharose column (1.2-ml columns; 2 mg Ig/ml CNBr-activated Sepharose 4B; Pharmacia Fine Chemicals, Uppsala, Sweden). Columns were extensively washed with 20 mM Tris-HCl, pH 7.5, containing 500 mM NaCl, 1 mM MgCl$_2$, 1 mM PMSF, and 0.1% NP-40 (wash buffer) and were eluted with 0.1% NP-40, 500 mM NaCl, and 1 mM PMSF in 200 mM acetic acid. The eluted fractions (0.8 ml) were neutralized with 0.25 ml of 1 M Tris-HCl, pH 8, and were analyzed quantitatively for Hermes antigens by dot-blot analysis (1-μl aliquots of serial dilutions of antigen preparations blotted on nitrocellulose and examined as described below for Western blots) and, in some experiments, by a sandwich-type ELISA (Hermes-1 as capture mAb and Hermes-3 as detection mAb; adapted from Staehelin et al., 1981). Antigen preparations to be used comparatively in a given experiment were quantified simultaneously, and the antigen concentration of each preparation was normalized by dilution to that of the least concentrated preparation.

For IEF and peptide mapping experiments, the eluted fractions with the highest Hermes antigen concentration (and corresponding fractions of normal rat IgG columns as controls) were labeled with ^{125}I using chloramine-T–mediated iodination (Klinman and Taylor, 1969). Labeled proteins were separated from free ^{125}I by precipitation with Hermes-1-Sepharose (or, for controls, normal rat IgG–Sepharose) followed by extensive washing over 10%/20% sucrose (in wash buffer) gradients and, finally, resuspension of beads in wash buffer.

For energy transfer experiments, Hermes antigens purified to near homogeneity (see Fig. 4) were conjugated to Texas red (TR) using the method of Titus et al. (1982). The unconjugated Hermes antigen preparations required for these experiments were treated identically except that TR was omitted. MAd was purified from mouse mesenteric lymph node stroma as previously described (Streeter et al., 1988a; Nakache et al., 1988) and conjugated to FITC using the method of Goding (1976). Murine MAd is appropriate for use in these experiments since lymphocyte-HEV interactions are not species specific, occurring with similar specificity and efficiency in xenogeneic and homologous combinations (Wu et al., 1988).

Electrophoretic Procedures and Western Blotting

Aliquots of crude lysates or purified Hermes antigen preparations were applied to 8% SDS-PAGE gels according to the method of Laemmli (1970). To preserve optimal antigenicity for Western blotting, samples were heated to 37°C for 15–30 min rather than boiling and gels were run under nonreducing conditions. Proteins were transferred to nitrocellulose with a trans-blot apparatus (Bio-Rad Laboratories, Richmond, CA). After blocking nonspecific protein binding with 100% horse serum for 30 min, primary and secondary antibody incubations (alkaline phosphatase-conjugated anti-rat IgG [Sigma Chemical Co., St. Louis, MO] or anti-mouse IgG [Promega Biotec, Madison, WI]) were done in a staining apparatus (Miniblotter 25; Immunetics, Cambridge, MA; for 1 h each). The alkaline phosphatase reaction was developed as described in the λ-gt11 screening kit (Promega Bio-

tec). For silver stain analysis, purified Hermes antigens were run on 10% SDS-PAGE gels under reducing conditions. Gels were fixed and stained per instructions of a silver stain kit (Bio-Rad Laboratories).

Slab gel IEF was done according to the method of Neefjes et al. (1986) using purified ^{125}I-labeled Hermes antigens (∿0.5 × 10⁶ cpm/lane). A standard surface electrode was used to measure the pH gradient formed in the gels. A ratio of ampholines (Pharmacia Fine Chemicals) of 50% pH 4–6.5, 33% pH 3–10, and 17% pH 3–5 gave the desired 4–7 pH gradient. Two-dimensional gel electrophoresis (IEF followed by SDS-PAGE) was performed as described by O'Farrell (1975).

Peptide mapping was done according to the method of Cleveland et al. (1977). The ^{125}I-labeled antigen preparations (∿0.5 × 10⁶ cpm/lane) were first run on preparative SDS-PAGE (8%, reducing conditions). These gels were dried unfixed, the desired bands were excised, and the gel slices were rehydrated before application to the Cleveland gels (12.5%). After the dye front was two thirds of the way through the stacking gel, the current was turned off and protease digestion using bovine pancreas trypsin (Sigma Chemical Co.; 7–30 μg/well in different experiments) or *Staphylococcal* V8 protease (Boehringer Mannheim GMB, Mannheim, FRG; 10–50 μg/well) was allowed to proceed for 40 min before the completion of the electrophoresis. Both IEF two-dimensional and Cleveland gels were fixed in 40% methanol, 10% acetic acid in distilled water, dried, and then exposed to X-OMAT AR film (Eastman Kodak Co., Rochester, NY) with an intensifying screen.

Hermes Antigen–MAd Binding Assay

Binding of Hermes antigens from different cell types to MAd was assessed using a technique based on the nonradiative transfer of fluorescence energy between closely associated fluorophores (Epe et al., 1983; Stryer, 1978, Nakache, M., E. L. Berg, L. J. Picker, and E. C. Butcher, manuscript submitted for publication). In this technique, the purified proteins to be assessed for binding interaction are conjugated to FITC (e.g., F-MAd) and to TR (e.g., TR-Hermes antigen), respectively. Under excitation at 493 nm, the FITC conjugate will give a characteristic emission spectrum peaking at ∿517 nm. Little or no emission is detected at 615 nm, the TR emission peak. If the proteins being tested do not interact, addition of the TR-conjugated species will not materially affect the FITC emission spectrum. On the other hand, if the FITC and TR conjugates do bind (i.e., approach to within ∿70 or less Å of each other), nonradiative (Forster) energy transfer will occur between the two fluorochromes (i.e., from FITC to TR). In this circumstance, the 517-nm emission of FITC will decrease (i.e., be quenched) and a 615-nm TR emission will appear.

We have defined a binding parameter δ which serves to quantitate the quenching of the 517-nm fluorescent emission due to energy transfer and to control for perturbations of the emission intensity due to conformational or electrostatic alterations associated with the addition of test or control solutions. The binding parameter

$$\delta = (F_o - F_q)/F_o,$$

where F_q and F_o represent the 517-nm emission after addition of a given amount of TR–Hermes antigen or an equal amount of unconjugated Hermes antigen, respectively. In other words, δ represents the fractional decrease in the 517-nm FITC emission due to the presence of the quencher/acceptor fluorophore (TR) on the Hermes antigen in complex with F-MAd. Thus, in these experiments, increasing amounts of the TR-labeled Hermes antigen preparations (<90 μl) were added to 200-μl aliquots of the F-MAd preparations, and the 517-nm emission was measured at 20°C on a fluorolog instrument (model 2000; Spectra-Physics, Inc., Mountain View, CA) with a spectral band width of 8 nm (493 nm excitation wavelength) after each addition (F_q). In parallel, similar measurements were made after the addition of equivalent amounts of unconjugated Hermes antigen to aliquots of the same F-MAd preparations (F_o).

For experiments assessing reversibility of gp90[Hermes]–MAd complexes, energy transfer was initially established with F-MAd and saturating amounts of KCA Hermes antigens (TR-labeled vs. unconjugated, as described above). The reaction mixtures were divided into five aliquots, and to each aliquot increasing amounts of unconjugated Hermes antigens from the five different cell types (equal amounts to cuvettes with TR-labeled and unconjugated KCA Hermes antigens) were added. The δ parameter was determined after each addition of unconjugated Hermes antigen. For antibody blocking experiments, 15 μg of Hermes-3, Hermes-1, or a class-matched mAb control for Hermes-3 was added to 150 μl of the Hermes antigen preparations (both TR-labeled and unconjugated) and allowed to incubate for 5–10 min before addition to F-MAd and calculation of δ as described

Table I. Distribution of Hermes Antigen in Nonhematolymphoid Human Tissues

Tissue type	Reactivity*
Epithelium/parenchymal organs	
Skin	
Epidermis	+
Sweat glands/pilosebaceous structures	+
Gastrointestinal tract	
Buccal/esophageal mucosa	+
Gastric/small and large intestinal mucosa	+‡
Pancreatic ducts/acini	+
Salivary gland ducts/acini	+
Liver	
Hepatocytes	−
Bile ducts	−
Kupffer cells	+
Kidney	
Bowman's capsule epithelium	−
Tubular epithelium	−
Mesangial cells	+
Lung	
Bronchial epithelium	±
Alveolar lining epithelium	+
Heart	
Myocardium	−
Breast	
Ducts and acini	+
Uterus	
Endometrial glands	+
Ovary	
Follicles	+
Testes	
Sertoli cells	−
Spermatozoa	−
Prostate	
Glands	+
Endocrine glands	
Thyroid follicular cells	+
Adrenal cortex	−
Adrenal medulla	+
Mesenchymal tissues	
Fibroblasts	+
Smooth muscle	
non-vascular	+
vascular	+ (Variable)
Endothelium	−
Skeletal muscle	
myocytes	±
endomysial cells	+
Nervous system	
Central	
glia	+ (Variable)
neurons	−
Peripheral	
Schwann cells	+ (Variable)

* Reactivity with Hermes-1, -2, and -3; H2-7; and H3-51 antibodies: (+) clear, unequivocal staining; (±) weak or equivocal staining; and (−) lack of reactivity above background.
‡ Staining is strongest at base of crypts and decreases towards superficial mucosa.

above. Characterization of MAd interaction with KCA and TL gp90[Hermes] by energy transfer has been previously reported (Nakache, M., E. L. Berg, L. J. Picker, and E. C. Butcher, manuscript submitted for publication) and is recapitulated in this report for purposes of comparison.
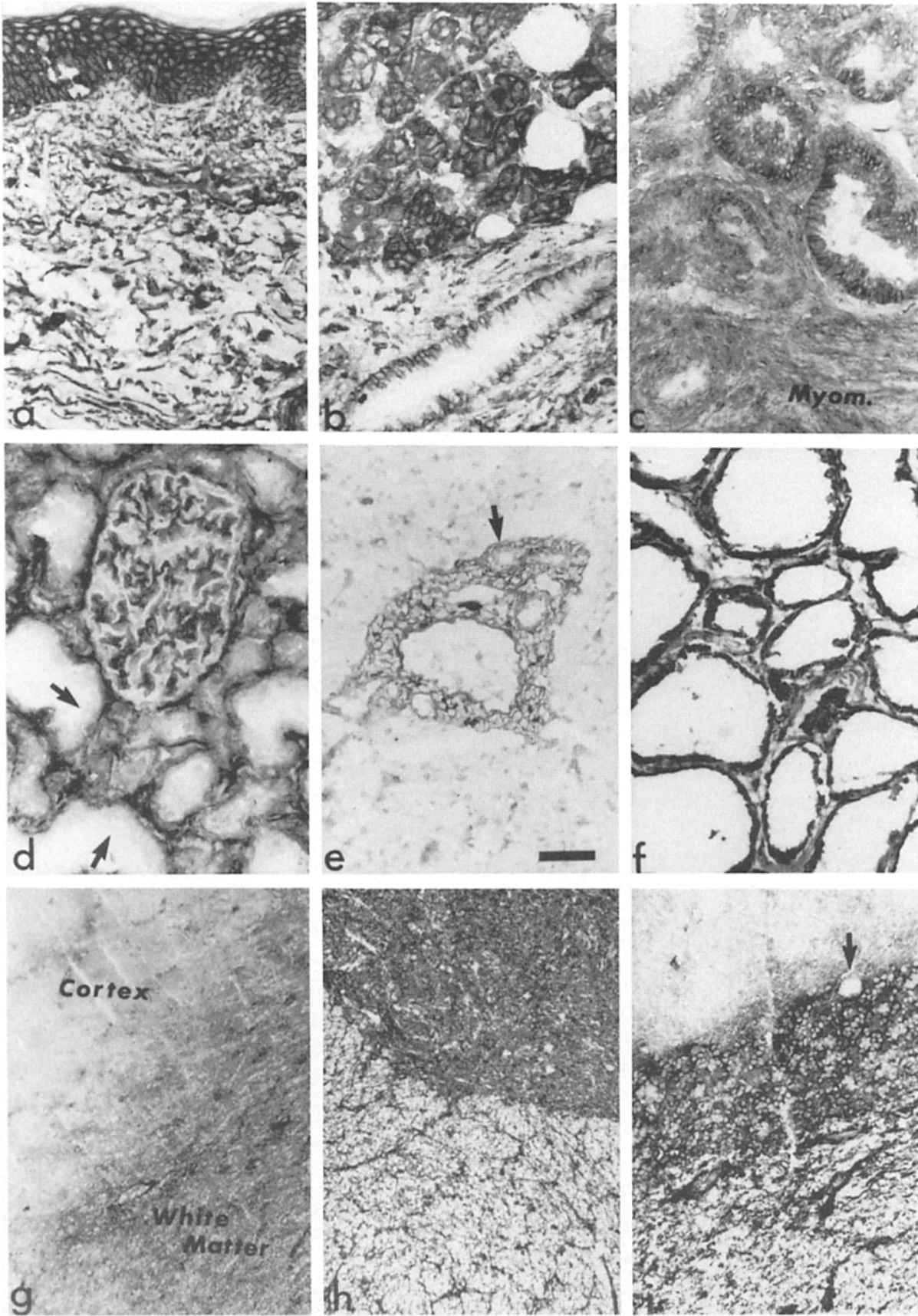
Figure 1. Distribution of Hermes antigen in normal human tissues (immunoperoxidase with methylene blue counterstain). (*a*) Skin section showing strong reactivity with epidermis (excluding stratum corneum) and dermal fibroblasts. A positive eccrine duct is present in the lower left corner. (*b*) Salivary gland section showing positive acini (*upper half*), a longitudinally sectioned duct (*lower half*; note that the

Results

Expression of Hermes Antigen in Normal Human Tissues

Immunohistologic examination of normal, nonhematolymphoid human tissues showed widespread expression of Hermes antigen (summarized in Table I). Five different mAbs, each to a distinct epitope on the lymphocyte gp90 molecules (including three antibodies whose epitopes are not dependent on posttranslational processing) were used in this study to rule out cross-reactivity with unrelated proteins. The different Hermes antibodies varied in staining intensity, but all showed the same pattern of reactivity in all tissues examined.

Squamous epithelia, both nonkeratinizing and keratinizing (Fig. 1 a), and most glandular epithelia (Fig. 1, b and c) showed strong expression of Hermes antigen. Some specialized epithelial cells, such as renal tubular cells (Fig. 1 d) and hepatocytes (Fig. 1 e), lacked Hermes antigen expression while others, such as thyroid follicular cells (Fig. 1 f), were positive. In general, staining was most intense in the germinative region of the epithelium (e.g., crypts of intestinal mucosa), and in simple ductal epithelium staining was often most intense abluminally and at the lateral cell borders (Fig. 1 b).

Among mesenchymal cells, fibroblasts and nonvascular smooth muscle cells appeared uniformly Hermes antigen positive (Fig. 1, a–d). Hermes antigen expression in vascular smooth muscle was variable with some vessels — particularly in the pulmonary circulation — showing little or no reactivity, while other vessels were strongly positive. Endothelium lacked reactivity, and staining of skeletal and cardiac muscle was either negative or equivocal.

In the central nervous system, a subset of glial cells, particularly fibrous astrocytes, were strongly Hermes antigen positive, whereas neurons and their processes appeared to be negative (Fig. 1, g–i). Staining was particularly intense in white matter (especially perivascular astrocytes; Fig. 1, g and i), subpial astrocytes, the granule cell layer in the cerebellum (Fig. 1 i), and the spinal cord grey matter (especially anterior horn; Fig. 1 h). Normal cortical glia were negative, whereas relatively fainter staining was observed in deep grey structures. In the peripheral nervous system, a subset of Schwann cells was intensely Hermes antigen positive.

Consistent with the observed patterns of reactivity in tissue sections, HFF, the squamous epithelial cell line SCL-1, and the glioma cell line HS-683 showed cell surface reactivity with Hermes-3 (Fig. 2) as well as the other mAbs of the Hermes series (not shown). The lymphoid cell line KCA also demonstrated surface staining with all Hermes mAbs (not shown). These cell lines were used as sources of cell type-specific Hermes antigen for the biochemical and functional studies discussed below.

Biochemical Characterization of Hermes Glycoproteins of Distinct Tissue Origin

Western blot analyses of crude lysates from human glioma cell line HS683, squamous epithelial cell line SCL-1, in vitro–passaged foreskin fibroblasts (HFF), lymphoid cell line KCA, and TL were used initially to compare the molecular properties of Hermes antigen derived from distinct cell types (Fig. 3). Using the Hermes-3 mAb on blots of HS683, HFF, KCA, and TL lysates, we demonstrated the presence of a major specific band in the 75–95-kD region (nonreducing conditions). In contrast to the aforementioned cell types, the squamous epithelial cell line SCL-1 showed a major broad band in the 140–190-kD region and only a very faint band at 80–90 kD. MAbs Hermes-1, Hermes-2, H2-7, and H3-51 gave similar results (not shown).

The Hermes-3 antibody was also used to probe Western blots of affinity-isolated Hermes antigens (Fig. 4). Again, HS683, HFF, and KCA demonstrated a major broad band in the 75–90-kD region. However, with the purified antigen preparations, a faint 210–220-kD band, which was not discernable in the analysis of crude lysates, was also identified in these cell types. The major SCL-1 band was at 140–160 kD and was clearly distinct from the 210–200-kD form. A faint band was discernable in the 80–90-kD region of the purified SCL-1 Hermes antigen preparations (similar to the major species of the other cell types). The trail-off of Hermes-3 reactivity in the 90–200-kD and 160–190-kD regions of the HS683 and SCL-1 crude lysates, respectively (Fig. 3), is probably due to incomplete reaction of the high protein crude lysates with SDS under the gentle reaction conditions used (purified antigen lacked most of this reactivity; cf. Fig. 4).

To further compare the molecular structure of Hermes glycoproteins from these different cell types, the purified antigen preparations were labeled with ^{125}I and subjected to slab gel IEF. As shown in Fig. 5, Hermes antigen from HS683, HFF, KCA, and TL focused similarly (pI ∼5.8). The 210–220-kD form does not iodinate efficiently and is not seen in these gels. The squamous epithelial cell line SCL-1 showed two bands after focusing — a minor band that comigrates with the Hermes antigens in the other cell types and a major, more basic band (pI ∼6.1). Two-dimensional gels (IEF followed by SDS-PAGE) confirmed that the more basic species corre-

---

reactivity is restricted to abluminal and lateral aspects of the epithelial cells), and fibroblasts (*lower half, adjacent to duct*). (*c*) Section of uterus showing positive endometrial glands and stroma (*upper half*) and positive smooth muscle cells in the myometrium (*Myom.*). (*d*) Kidney section showing Hermes reactivity in mesangial cells within the glomerulus and in interstitial fibroblasts; Bowman's capsule epithelial cells and tubular epithelial cells (*arrows*) are negative. (*e*) Liver section showing reactivity in portal fibroblasts and scattered Kuppfer cells within the hepatic lobule. Hepatocytes and bile duct epithelium (*arrow*) are negative. (*f*) Section of thyroid demonstrating strong staining of thyroid follicles. (*g*) Section of brain demonstrating extensive reactivity in subcortical white matter (note perivascular enhancement) and lack of reactivity in neocortex. (*h*) Section of spinal cord showing strong positivity of both white matter (*lower half*) and anterior horn grey matter (*upper half*). (*i*) Section of cerebellum showing Hermes reactivity in white matter (*lower third*; again note perivascular accentuation) and granular cell layer (*middle third*; granular layer neurons and Purkinje cells [*arrow*] appear negative; positivity is attributable to interspersed glia) and lack of reactivity in molecular layer (*upper third*). Bar: (*a–f* and *i*) 60 μm; (*g*) 120 μm; (*h*) 200 μm.
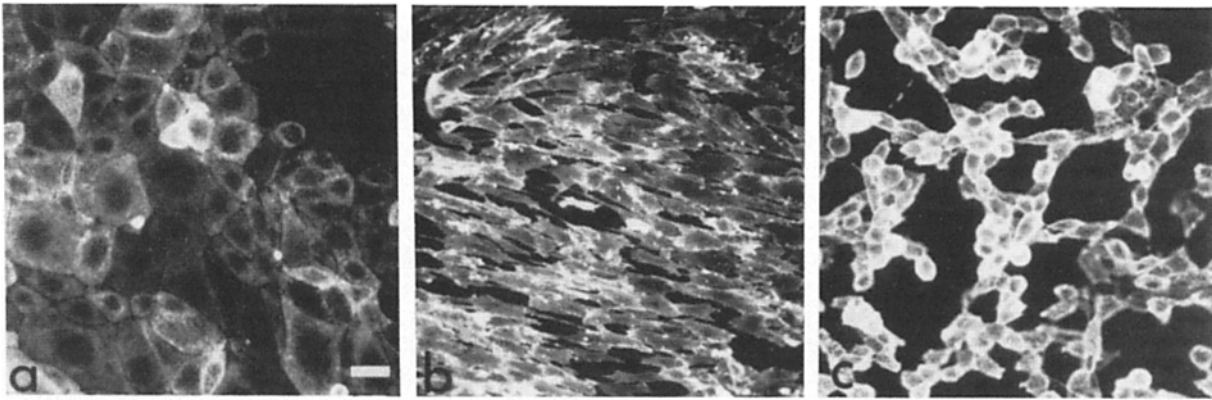
Figure 2. Demonstration by immunofluorescence of cell surface Hermes-3 reactivity on (*a*) the squamous epithelial cell line SCL-1; (*b*) HFF; and (*c*) glial cell line HS683. Bar, 20 μm.

sponds to the 140–160-kD polypeptide and that the more acidic species corresponds to the 80–90-kD polypeptide (not shown).

The biochemical similarity of the 75–90-kD Hermes antigens from all the different cell types was substantiated by peptide mapping using the technique of Cleveland et al.
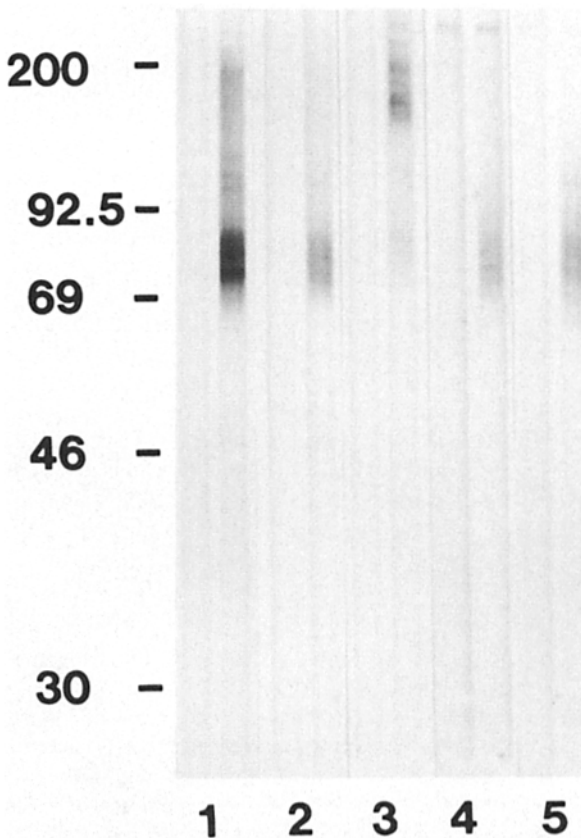

Figure 3. Western blot analysis of crude lysates with Hermes-3 (*right lane each column*) vs. class-matched control (*left lane each column*). HS683 (column *1*), HFF (column *2*), TL (column *4*), and KCA (column *5*) show predominant specific bands in the 75–90-kD region, whereas SCL-1 (column *3*) shows only a faint band in this region and a major specific band at 140–190 kD (8% SDS-PAGE, nonreducing). A nonspecific band in the 220-kD region of the gel is present in the TL lysates (column *4*).

(1977) (Fig. 6). Preparative SDS-PAGE was used to isolate each band before analysis. All of the 75–90-kD species, including the minor SCL-1 80–90-kD band, yielded identical degradation products after digestion with V8 protease or trypsin. V8 protease treatment resulted in a major 25–30-kD degradation product, whereas the major tryptic fragment was 40 kD. The 140–160-kD major SCL-1 band, when tested under identical conditions, appeared much more protease resistant than the lower molecular mass species. Trypsin failed to cleave this high molecular mass squamous epithelial band under the condition tested. V8 protease cleaved this species less efficiently than the 75–90-kD antigen, but did result in an identical 25–30-kD degradation product, suggesting some degree of molecular homology with the lower molecular mass form.

Functional Comparison of Hermes Glycoproteins from Different Cell Types

We have previously shown a specific binding interaction between isolated MAd and KCA-derived Hermes glycoproteins using a technique based on the nonradiative transfer of electronic energy between donor and acceptor fluorochromes (Nakache, M., E. L. Berg, L. J. Picker, and E. C. Butcher, manuscript submitted for publication). To ask whether the Hermes antigens from nonlymphoid cell types were functionally, as well as structurally, homologous to lymphocyte homing receptors, we assessed their capacity to interact with MAd. As shown in Fig. 7, Hermes antigen derived from HS683 and HFF (predominantly 75–90 kD) did indeed bind MAd, whereas SCL-1 Hermes antigen (predominantly 140–160 kD) demonstrated little, if any, interaction. Interestingly, glial- and lymphocyte-derived Hermes molecules showed plateau δ values in the same range, whereas Hermes antigen isolated from fibroblasts demonstrated a considerably lower maximum δ. These differences were not due to variation in the TR-labeling of the different Hermes preparations since reversal experiments, in which preformed MAd–Hermes$_{KCA}$ complexes were competitively disrupted with increasing amounts of unconjugated Hermes antigen from the different cell types, showed generally similar results (Fig. 8). Furthermore, the differences in the binding characteristics of Hermes antigens of different cellular origin were observed with two independent preparations of Hermes antigen from each cell type.
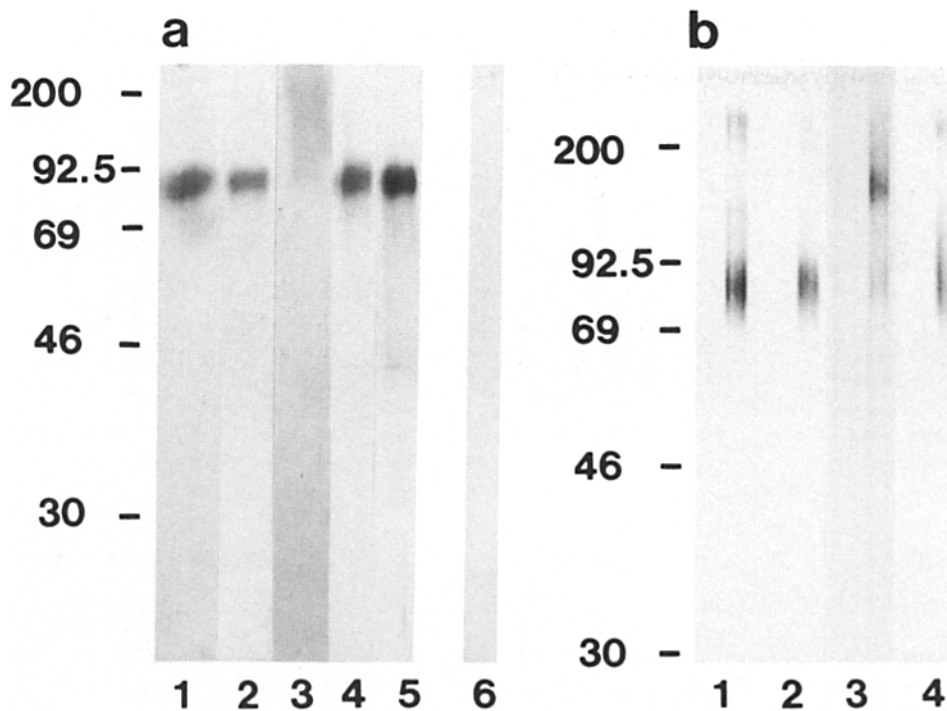
a

200 —
92.5—
69 —
46 —
30 —

1 2 3 4 5 6

b

200 —
92.5—
69 —
46 —
30 —

1 2 3 4

Figure 4. (*a*) Silver-stained SDS-PAGE gels (10%, reducing) of isolated Hermes antigens from HS683 (lane *1*), HFF (lane *2*), SCL-1 (lane *3*), TL (lane *4*), and KCA (lane *5*) showing purity of these preparations. Lane *6* is a representative eluate (corresponding to peak fractions of specific columns) from control antibody (normal rat IgG) precolumn. (*b*) Western blot analysis of purified Hermes preparations with Hermes-3 (*right lane each column*) vs. class-matched control antibody (*left lane each column*). HS683 (column *1*), HFF (column *2*), and TL (column *4*) show major 75–90-kD and faint 210–220-kD specific bands. In contrast, SCL-1 (column *3*) shows a faint 75–90-kD and a major 140–160-kD specific band (8% SDS-PAGE, nonreducing).

Lymphocyte binding to mucosal HEV and lymphocyte gp90^{Hermes} binding to isolated MAd is blocked by the Hermes-3 antibody (Jalkanen et al., 1987; Nakache, M., E. L. Berg, L. J. Picker, and E. C. Butcher, manuscript submitted for publication). In contrast, the Hermes-1 antibody, which recognizes a distinct epitope on gp90^{Hermes}, does not block lymphocyte binding to HEV of any specificity (Jalkanen et al., 1986*b*) and shows only limited ability to interfere with lymphocyte gp90^{Hermes}–MAd interaction as measured by energy transfer (Nakache, M., E. L. Berg, L. J. Picker, and E. C. Butcher, manuscript submitted for publication).

Figure 5. IEF gel of isolated Hermes molecules from KCA (lane *1*), HS683 (lane *2*), HFF (lane *3*), SCL-1 (lane *4*), and TL (lane *5*). The 75–90-kD molecules show identical isoelectric points, whereas the major 140–160-kD SCL-1 is slightly more basic. The narrow bands seen near the bottom of the gel in lanes *1* and *2* represent acidic spontaneous breakdown products noted to occur in some preparations with time.

As shown in Fig. 9, analogous results are observed with HS683 (glial)-derived gp90^{Hermes}. Hermes-3, but not Hermes-1 or an isotype-matched nonbinding control antibody, blocked the interaction between HS683 Hermes antigen and MAd.

Discussion

The Hermes-defined lymphocyte cell surface glycoproteins have been designated lymphocyte homing receptors on the basis of their role in lymphocyte recognition of HEV. The participation of this class of molecules in lymphocyte HEV recognition and lymphocyte homing is supported by several lines of experimental evidence. First, lymphoid cell lines lacking these glycoproteins generally bind HEV poorly or not at all (Jalkanen et al., 1986*a,b*). Second, antibodies reactive with this class of molecules can block binding to HEV. For example, mAb Hermes-3 blocks lymphocyte binding to mucosal HEV, and polyclonal anti–Hermes-1 antigen antiserum blocks lymphocyte binding to all HEV types (Jalkanen et al., 1987). Third, as described above, purified Hermes molecules from TL and the mucosal HEV-specific cell line KCA specifically bind the high endothelial cell surface protein MAd (Nakache, M., E. L. Berg, L. J. Picker, and E. C. Butcher, manuscript submitted for publication). While these data establish that Hermes glycoproteins are involved in lymphocyte recognition of HEV, the results presented in this report suggest this class of molecules may have much broader functional significance, perhaps constituting a novel family of primary CAMs.

Our finding that glycoproteins closely related to lymphocyte homing receptors are widely expressed in the human body (including cells derived from all three primary germ layers) confirm and extend previous observations showing CD44 antigen expression in normal brain, kidney, breast, and colon, as well as a variety of cell lines and tumors de-
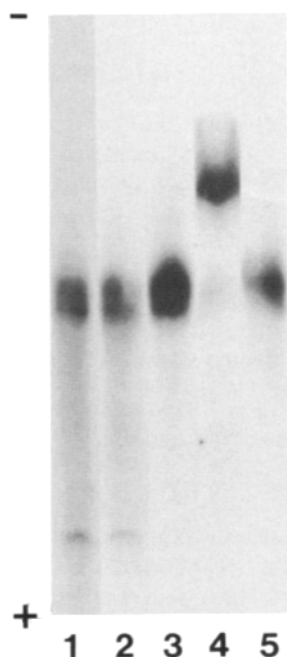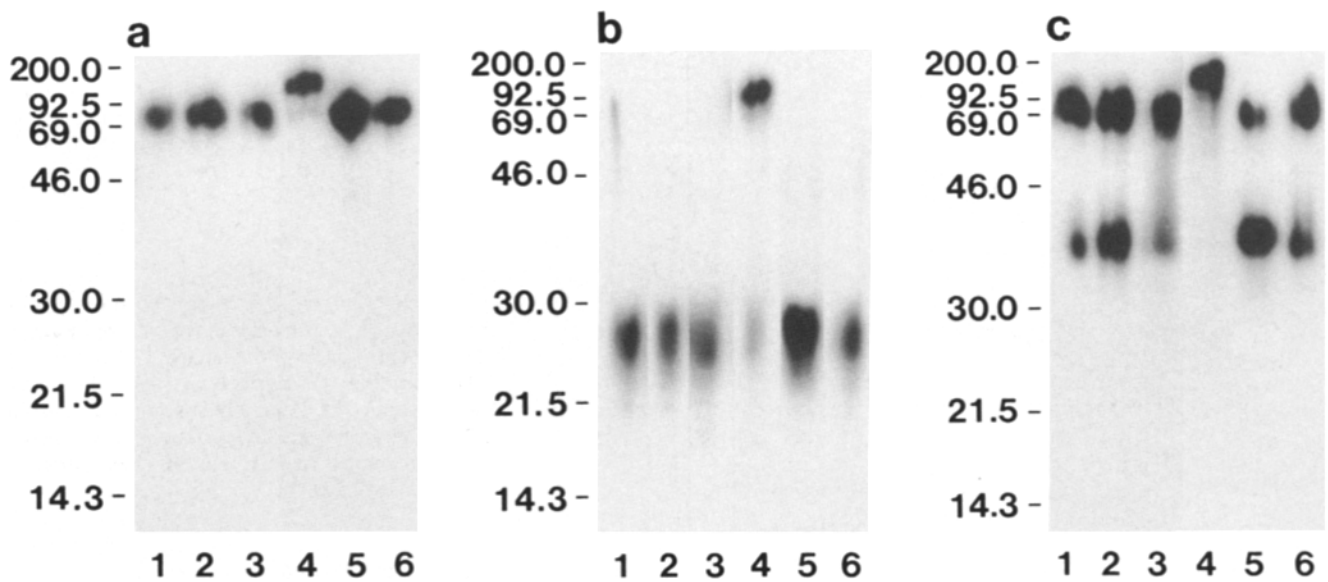
Figure 6. Cleveland gels of isolated Hermes 75–90-kD molecules derived from KCA (lane *1*), HS683 (lane *2*), SCL-1 (lane *3*), HFF (lane *5*), and TL (lane *6*) and of the isolated 140–160-kD SCL-1 species (lane *4*). (*a*) Without added protease; (*b* and *c*) contained 30 μg/well V8 protease and 50 μg/well trypsin, respectively. All species yielded a major V8 degradation product of 25–30 kD, whereas only the 75–90-kD forms showed the 40-kD trypsin degradation product. The 40-kD tryptic fragment was not observed in the lane with the 140–160-kD SCL-1 antigen even after prolonged exposure times.
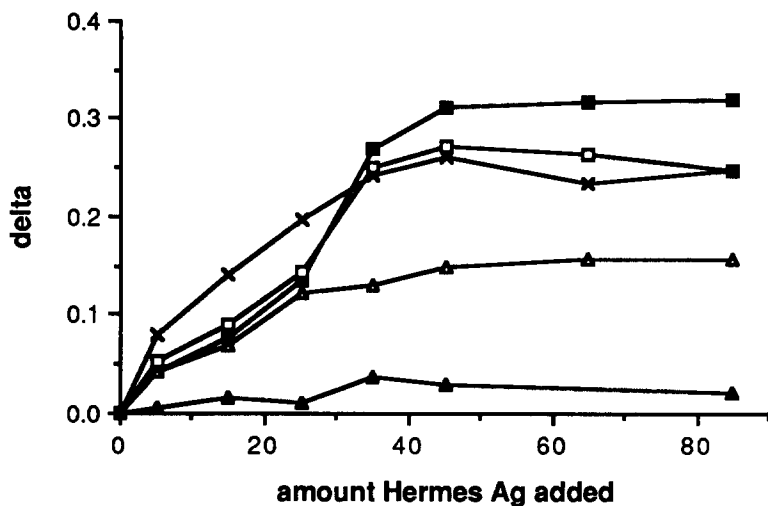
Figure 7. Direct assessment of MAd binding by Hermes antigen isolated from the KCA lymphoid cell line (□), TL (■), HS683 glial cell line (X), HFF (△), and SCL-1 squamous epithelial cell line (▲). Increasing amounts of Hermes antigen (unlabeled vs. TR conjugated) were added to identical solutions of F-MAd. All Hermes antigen preparations were at equivalent antigen concentrations. δ, a quantitative parameter related to the energy transfer–associated quenching of the 517-nm FITC emission due to binding of TR-labeled gp90 to F-MAd (see text), is plotted vs. the amount of Hermes antigen added (arbitrary units).
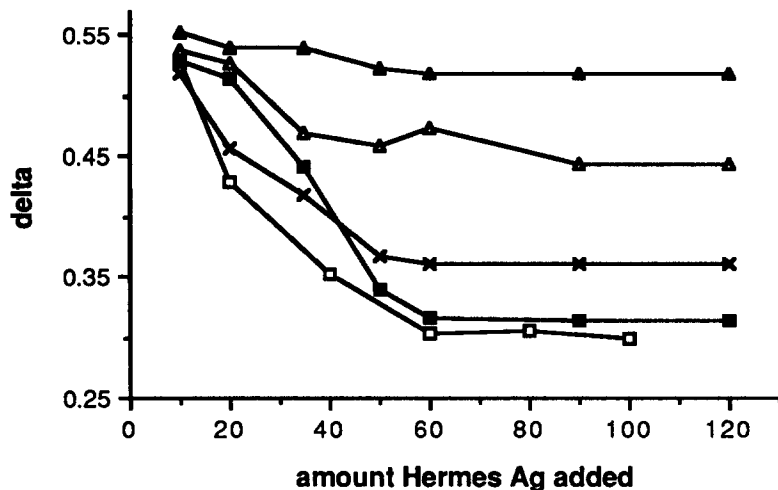

Figure 8. Reversal of preformed KCA Hermes antigen-MAd complexes by Hermes antigens of different origin. Plateau binding was established with gp90[Hermes] from the KCA lymphoid cell line (unlabeled vs. TR conjugated) as shown in Fig. 7. The reaction mixture was aliquoted and then increasing amounts of unlabeled Hermes antigen from the KCA cell line (□), TL (■), HS683 glial cell line (X), HFF (△), and SCL-1 squamous epithelial cell line (▲) were added. All Hermes antigen preparations were at equivalent antigen concentration. Results are presented as δ vs. the amount of competing unlabeled Hermes antigen added (arbitrary units).
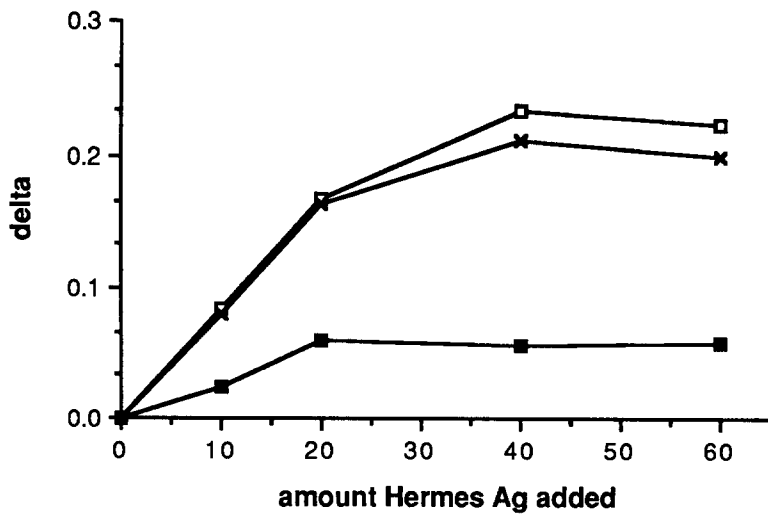
Figure 9. Antibody inhibition of the binding of glial gp90^Hermes to MAd. Hermes-3 (■), but not a class-matched nonbinding control antibody (□) or Hermes-1 (X), block fluorescence energy transfer when added to the glial gp90^Hermes preparations before incubation with F-MAd. Results are presented as δ vs. the amount of Hermes antigen (with antibody) added (arbitrary units).

rived from these and other sites (Letarte et al., 1985; Quackenbush et al., 1985, 1986; Daar and Fabre, 1981, 1983; McKenzie et al., 1982). Our study shows considerably more expression of the Hermes/CD44 antigen in central nervous system grey matter (e.g., spinal cord grey matter) than previously appreciated, as well as documenting expression in previously unreported sites (Table I). Five distinct homing receptor epitopes, including three that are not dependent on eukaryotic posttranslational processing, are coexpressed at all positive tissue sites, strongly suggesting that this broad distribution is not due to cross-reactivity of carbohydrate epitopes on dissimilar glycoproteins, as has been reported for the HNK-1/L2 and L3 antigens (Kruse et al., 1984; Kucherer et al., 1987).

Biochemical studies of Hermes antigens derived from disparate cell types also indicate that these various Hermes molecules are closely related. Three structurally distinct species of Hermes antigen were defined: 75–90, 140–160, and 210–220 kD. In a recent study using the CD44 mAb 50B4 and the Pgp-1-specific mAb E1/2, Omary et al. (1988) showed three probably analogous molecular species variably expressed on lymphoid, epithelial, and fibroblast cell lines, but did not further compare these molecules. In our comparison of these various species, we found that the 75–90-kD Hermes antigen (the major form of Hermes antigen on lymphoid cells, glial cells, and fibroblasts) from all the cell types examined had identical isoelectric points and peptide maps, consistent with strong structural homology, or perhaps even identity (see below), between these species. Lymphoid cells, glial cells, and fibroblasts also possessed a minor 210–220-kD Hermes antigen species, which in lymphoid cells has previously been shown to be a chondroitin-sulfate–modified form that appears to share a common precursor with the 75–90-kD species (Jalkanen et al., 1988). The major Hermes antigen in the squamous epithelial cell line SCL-1 was 140–160 kD, showed a more basic isoelectric point, and was resistant to trypsin. This 140–160-kD species did, however, express multiple Hermes epitopes and shared a common V8 protease degradation product with the 75–90-kD form, suggesting considerable structural homology between the two species. Chondroitinase, heparinase, and keratinase did not affect the 140–160-kD SCL-1 antigen, and digestion with

O-glycanase, N-glycanase, and neuraminidase, in combination and alone, showed relatively small effects, insufficient to account for the molecular mass difference with the 75–90-kD species (Picker, L., unpublished observations). Furthermore, pulse–chase experiments with radiolabeled methionine indicate that the earliest, lowest molecular mass Hermes antigen precursor from SCL-1 squamous epithelial cells is 15–20 kD larger than that of the other cell types (Uksila, J., and L. Picker, unpublished observations). Thus, while the exact nature of the structural differences between gp90^Hermes and gp150^Hermes is unclear, the larger size of gp150^Hermes must, at least in part, be due to additional primary sequence and/or to early posttranslational modifications that are not affected by the glycolytic enzymes described above.

These serologic and biochemical comparisons indicate a close structural relationship between the Hermes/CD44 antigens on diverse cell types, but do not directly address whether these antigens are functionally homologous as well. To examine this question, we took advantage of one known function of the Hermes class of lymphocyte homing receptor—its ability to bind MAd, an endothelial cell surface adhesion molecule for lymphocytes that directs lymphocyte homing to mucosal lymphoid tissues (Streeter et al., 1988a; Nakache et al., 1988; Nakache, M., E. L. Berg, L. J. Picker, and E. C. Butcher, manuscript submitted for publication). We found that isolated Hermes glycoproteins from such disparate cell types as fibroblasts and glial cells were able to bind MAd, whereas the structurally distinct squamous epithelial Hermes antigen lacked this binding activity. The ability of mAb Hermes-3, but not Hermes-1, to block the glial gp90^Hermes–MAd interaction (the same pattern of antibody inhibition seen for lymphocyte binding to mucosal HEV and direct lymphoid gp90^Hermes–MAd interaction) suggests that MAd binding by lymphoid and nonlymphoid gp90^Hermes is mediated by similar binding domains. The inability of gp150^Hermes to interact with MAd suggests that this binding domain is either absent or blocked in this higher molecular mass form. It is also important to note that the binding curves of the 75–90-kD Hermes antigens from lymphoid cells, glia, and fibroblasts to MAd were reproducibly different. This observation raises the possibility that functionally important structural differences exist between the 75–90-kD Hermes

antigens on different cell types that were not apparent in our biochemical analyses. In other systems, subtle structural alterations (e.g., single amino acid substitutions) have shown to dramatically alter binding specificities of proteins (Rogers et al., 1983; Mellins et al., 1988).

The specific interaction between MAd and nonlymphoid Hermes glycoproteins is not likely of physiologic significance per se, since MAd expression is largely limited to postcapillary venules in mucosal tissues (Streeter et al., 1988a). However, the ability of diverse gp90[Hermes] to interact with MAd implies that they too may be adhesion molecules, perhaps recognizing ligands homologous to MAd. In this context, it is interesting that rat lymphocytes specifically bind to white matter tracts in the rat brain in a manner that mimics lymphocyte binding to HEV (similar specificity for thoracic duct lymphocytes vs. thymocytes, similar temperature dependence, etc.; Kuttner and Woodruff, 1979). Given our present demonstration of high levels of gp90[Hermes] in white matter tracts and the remarkable ability of glial gp90[Hermes] to interact with a homing receptor ligand, such binding of lymphocytes to myelinated tracts could be mediated by cross-reactive binding of rat gp90 homing receptors to a native ligand for glial gp90 in white matter.

Ligands for nonlymphoid Hermes glycoproteins need not structurally resemble MAd to any great degree. For example, gp90[Hermes] has been implicated in lymphocyte recognition of peripheral lymph node HEV (Jalkanen et al., 1987). Although not yet formally proven, the putative endothelial ligand for this binding interaction is the peripheral lymph node addressin (Streeter et al., 1988b; Streeter, P. R., L. J. Picker, S. A. Michie, and E. C. Butcher, manuscript in preparation), a 90-kD glycoprotein with structural characteristics distinct from MAd (Berg et al., 1989).

As mentioned above, we have recently demonstrated that the Hermes, CD44 (In[Lu]-related p80), and human Pgp-1 antigens are similar or perhaps identical (Picker et al., 1989), and Gallatin, W. M., E. Wayner, T. St. John, E. C. Butcher, and W. Carter (manuscript submitted for publication) have recently suggested close homology or identity between these molecules and the extracellular matrix receptor III described by Carter and Wayner (1988). No function has previously been attributed to CD44 and human Pgp-1; however, the extracellular matrix receptor III has been implicated in the adhesion of fibroblasts to extracellular matrix components including collagen (Carter and Wayner, 1988). Furthermore, preliminary studies suggest that the lymphocyte Hermes antigen can interact with fibronectin and collagen (Jalkanen, S., personal communication). These observations suggest that gp90[Hermes] may have several binding specificities, perhaps mediated by distinct binding domains. In this context, it is of interest that N-CAM, the prototypical primary CAM, has two binding activities mediated by distinct domains on the N-CAM molecule(s): a homophilic binding site responsible for cell–cell interaction and a heparin-sulfate–binding site, presumably mediating extracellular matrix binding (Cole and Glaser, 1986). Furthermore, recent sequence analysis of gp90[Hermes] encoding cDNAs from KCA has revealed a striking homology to domains in cartilage proteoglycan core and link proteins (Goldstein et al., 1989) that may interact bifunctionally with hyaluronic acid and protein (Neame et al., 1987; Goetinck et al., 1987).

The Hermes antigens, like other primary adhesion mole-

cules (Crossin et al., 1985; Hatta et al., 1987), also appear to be dynamically expressed during development. For example, in a separate immunohistologic study of the developing human central nervous system, we have identified Hermes antigen expression on radial glia in the germinal matrix of fetal brains and have noted that the appearance of Hermes antigen expression in central nervous system white matter appears to precede or accompany the process of myelination (Vogel, H., L. Picker, and E. Butcher, manuscript in preparation). McKenzie et al. (1982) have also noted that the amount of CD44 antigen markedly increases in brain during development.

Taken together, these data strongly suggest that the Hermes-defined cell surface molecules constitute a closely related family of CAMs, likely involved in diverse cell–cell or cell–matrix interactions in cooperation with other cell adhesion systems. Given that one of the first reported adhesion/ recognition functions for these glycoproteins was in the process of lymphocyte homing, we have designated these molecules homing-CAMs (H-CAM). In the case of lymphocyte-HEV interaction there is increasing evidence that a number of distinct CAMs act in concert to control the specificity of lymphocyte homing (Berg et al., 1989). However, as shown in this report, Hermes-defined H-CAMs appear functionally heterogenous, and this heterogeneity could also contribute to or reflect specificity of function in diverse cell–cell or cell–matrix interactions. The molecular basis of H-CAM heterogeneity is largely unexplained, but in this regard studies of genomic DNA with the recently isolated H-CAM encoding cDNAs are compatible with one, or at most two, H-CAM genes (Goldstein et al., 1989). This observation suggests that H-CAM structural and functional heterogeneity is likely generated either by alternative RNA processing or by differential posttranslational modification, processes previously demonstrated to be important in generating functional variants of other CAMs (Cunningham et al., 1987; Hoffman and Edelman, 1983; Rougon et al., 1982). Additional studies will be required to define in detail the role or roles of the H-CAM molecular family in the development and function of nonlymphoid tissues.

References

Berg, E. L., L. A. Goldstein, M. A. Jutila, M. Nakache, L. J. Picker, P. R. Streeter, N. W. Wu, D. Zhou, and E. C. Butcher. 1989. Homing receptors and vascular addressins: cell adhesion molecules that direct lymphocyte traffic. Immunol. Rev. 108:5–18.

Bindl, J. M., and R. A. Warnke. 1986. Advantages of detecting monoclonal antibody binding to tissue sections with biotin and avidin reagents in coplin jars. Am. J. Clin. Pathol. 85:490–493.

Boukamp, P., W. Tilgen, R. T. Dzarlieva, D. Breitkreutz, D. Haag, R. K.

Riehl, A. Bohnert, and N. E. Fusenig. 1982. Phenotypic and genotypic characteristics of a cell line from a squamous cell carcinoma of human skin. *J. Natl. Cancer Inst.* 68:415–427.

Carter, W. G., and E. A. Wayner. 1988. Characteristics of the class III collagen receptor, a phosphorylated, transmembrane glycoprotein expressed in nucleated human cells. *J. Biol. Chem.* 263:4193–4201.

Cleveland, D. W., S. G. Fischer, M. W. Kirschner, and U. K. Laemmli. 1977. Peptide mapping by limited proteolysis in sodium dodecyl sulfate and analysis by gel electrophoresis. *J. Biol. Chem.* 252:1102–1106.

Cole, G. J., and L. Glaser. 1986. A heparin-binding domain from N-CAM is involved in neural cell-substrate adhesion. *J. Cell Biol.* 102:403–412.

Crossin, K. L., C.-M. Chuong, and G. M. Edelman. 1985. Expression sequences of cell adhesion molecules. *Proc. Natl. Acad. Sci. USA.* 82:6942–6946.

Cunningham, B. A., J. J. Hemperly, B. A. Murray, E. A. Prediger, R. Brackenbury, and G. M. Edelman. 1987. Neural cell adhesion molecule: structure, immunoglobulin-like domains, cell surface modulation, and alternative RNA splicing. *Science (Wash. DC).* 236:799–806.

Daar, A. S., and J. W. Fabre. 1981. Demonstration with monoclonal antibodies of an unusual mononuclear cell infiltrate and loss of normal epithelial membrane antigens in human breast carcinomas. *Lancet.* 2:434–438.

Daar, A. S., and J. W. Fabre. 1983. The membrane antigens of human colorectal cancer cells: demonstration with monoclonal antibodies of heterogeneity within and between tumours and of anomalous expression of HLA-DR *Eur. J. Cancer & Clin. Oncol.* 19:209–220.

Dustin, M. L., R. Rothlein, A. K. Bhan, C. A. Dinarello, and T. A. Springer. 1986. Induction by IL-1 and interferon-gamma: tissue distribution, biochemistry, and function of a natural adherence molecule (ICAM-1). *J. Immunol.* 137:245–254.

Edelman, G. M., and J. P. Thiery, editors. 1985. The Cell in Contact: Adhesion and Junctions as Morphogenetic Determinants. John Wiley & Sons Inc., New York. 507 pp.

Epe, B., K. G. Steinhauser, and P. Woolley. 1983. Theory of measurement of Forster-type energy transfer in macromolecules. *Proc. Natl. Acad. Sci. USA.* 80:2579–2583.

Goding, J. W. 1976. Conjugation of antibodies with fluorochromes: modifications to the standard methods. *J. Immunol. Methods.* 13:215–226.

Goetinck, P. F., N. S. Stirpe, P. A. Tsonis, and D. Carlone. 1987. The tandemly repeated sequences of cartilage link protein contain sites for interaction with hyaluronic acid. *J. Cell Biol.* 105:2403–2408.

Goldstein, L. A., D. F. H. Zhou, L. J. Picker, C. N. Minty, R. F. Bargatze, J. F. Ding, and E. C. Butcher. 1989. A human lymphocyte homing receptor, the Hermes antigen, is related to cartilage proteoglycan core and link proteins. *Cell.* 56:1063–1072.

Hatta, K. S., S. Takagi, H. Fujisawa, and M. Takeichi. 1987. Spatial and temporal expression pattern of N-cadherin cell adhesion molecules correlated with morphogenetic processes of chicken embryos. *Dev. Biol.* 120:215–227.

Haynes, B. F., L. L. Hensley, and B. V. Jegasothy. 1982. Differentiation of human T lymphocytes. II. Phenotypic difference in skin and blood malignant T-cells in cutaneous T-cell lymphoma. *J. Invest. Dermatol.* 78:323–326.

Hoffman, S., and G. M. Edelman. 1983. Kinetics of homophilic binding by embryonic and adult forms of the neural cell adhesion molecule. *Proc. Natl. Acad. Sci. USA.* 80:5762–5766.

Isacke, C. M., C. A. Sauvage, R. Hyman, J. Lesley, R. Schulte, and I. S. Trowbridge. 1986. Identification and characterization of the human Pgp-1 glycoproteins. *Immunogenetics.* 23:326–332.

Jalkanen, S., R. A. Reichert, W. M. Gallatin, R. F. Bargatze, I. L. Weissman, and E. C. Butcher. 1986a. Homing receptors and the control of lymphocyte migration. *Immunol. Rev.* 91:39–60.

Jalkanen, S., R. F. Bargatze, L. Herron, and E. C. Butcher. 1986b. A lymphoid cell surface glycoprotein involved in endothelial cell recognition and lymphocyte homing in man. *Eur. J. Immunol.* 16:1195–1202.

Jalkanen, S., R. F. Bargatze, J. de los Toyos, and E. C. Butcher. 1987. Lymphocyte recognition of high endothelium: antibodies to distinct epitopes of an 85-95-kD glycoprotein antigen differentially inhibit lymphocyte binding to lymph node, mucosal, or synovial endothelial cells. *J. Cell Biol.* 105: 983–990.

Jalkanen, S., M. Jalkanen, R. F. Bargatze, M. Tammi, and E. C. Butcher. 1988. Biochemical properties of glycoproteins involved in lymphocyte recognition of high endothelial venules in man. *J. Immunol.* 141:1615–1623.

Jessell, T. M. 1988. Adhesion molecules and the hierarchy of neural development. *Neuron.* 1:3–13.

Klinman, N. R., and R. B. Taylor. 1969. General methods for the study of cells and serum during the immune response: the response to dinitrophenyl in mice. *Clin. Exp. Immunol.* 4:473–487.

Kruse, J., R. Mailhammer, H. Wernecke, A. Faissner, I. Sommer, C. Goridis, and M. Schachner. 1984. Neural cell adhesion molecules and myelin-associated glycoprotein share a common carbohydrate moiety recognized by monoclonal antibodies L2 and HNK-1. *Nature (Lond.).* 311:153–155.

Kucherer, A., A. Faissner, and M. Schachner. 1987. The novel carbohydrate epitope L3 is shared by some neural cell adhesion molecules. *J. Cell Biol.* 104:1597–1602.

Kuttner, B. J., and J. J. Woodruff. 1979. Selective adherence of lymphocytes to myelinated areas of rat brain. *J. Immunol.* 122:1666–1671.

Laemmli, U. K. 1970. Cleavage of structural proteins during the assembly of the head of bacteriophage T4. *Nature (Lond.).* 227:680–685.

Letarte, M., S. Iturbe, and E. J. Quackenbush. 1985. A glycoprotein of molecular weight 85,000 on human cells of B-lineage: detection with a family of monoclonal antibodies. *Mol. Immunol.* 22:113–124.

McKenzie, J. L., R. Dalchau, and J. W. Fabre. 1982. Biochemical characterization and localization in brain of a human brain-leucocyte membrane glycoprotein recognized by a monoclonal antibody. *J. Neurochem.* 39:1461–1466.

Mellins, E., B. Arp, B. Ochs, H. Erlich, and D. Pious. 1988. A single amino acid substitution in the human histocompatibility leukocyte antigen DR3 β chain selectively alters antigen presentation. *J. Exp. Med.* 168:1531–1537.

Nakache, M., E. L. Berg, P. R. Streeter, and E. C. Butcher. 1988. The mucosal vascular addressin is a tissue-specific endothelial cell molecules for circulating lymphocytes. *Nature (Lond.).* 337:179–181.

Neame, P. J., J. E. Christner, and J. R. Baker. 1987. Cartilage proteoglycan aggregates: the link protein and proteoglycan amino-terminal globular domains have similar structures. *J. Biol. Chem.* 262:17768–17778.

Neefjes, J. J., I. Doxiadis, N. J. Stam, C. J. Beckers, and H. L. Ploegh. 1986. An analysis of class I antigens of man and other species by one-dimensional IEF and immunoblotting. *Immunogenetics.* 23:164–171.

Obrink, B. 1986. Epithelial cell adhesion molecules. *Exp. Cell Res.* 163:1–21.

O'Farrell, P. H. 1975. High resolution two-dimensional gel electrophoresis. *J. Biol. Chem.* 250:4007–4021.

Omary, M. B., I. S. Trowbridge, M. Letarte, M. F. Kagnoff, and C. M. Isacke. 1988. Structural heterogeneity of human Pgp-1 and its relationship with p85. *Immunogenetics.* 27:460–464.

Picker, L. J., J. de los Toyos, M. J. Telen, B. F. Haynes, and E. C. Butcher. 1989. Monoclonal antibodies against the CD44 (In[Lu]-related p80) and Pgp-1 antigens in man recognize the Hermes class of lymphocyte homing receptors. *J. Immunol.* 142:2046–2051.

Quackenbush, E. J., T. F. Cruz, M. A. Moscarello, and M. Letarte. 1985. Identification of three antigens in human brain associated with similar antigens on human leukaemic cells. *Biochem. J.* 225:291–299.

Quackenbush, E. J., A. Gougos, R. Baumal, and M. Letarte. 1986. Differential localization within human kidney of five membrane proteins expressed on acute lymphoblastic leukemia cells. *J. Immunol.* 136:118–124.

Rogers, G. N., J. C. Paulson, R. S. Daniels, J. J. Skehel, I. A. Wilson, and D. C. Wiley. 1983. Single amino acid substitutions in influenza haemagglutinin change receptor binding specificity. *Nature (Lond.).* 304:76–78.

Rougon, G., H. Deagostini-Bazin, M. Hirn, and C. Goridis. 1982. Tissue- and developmental stage-specific forms of a neural cell surface antigen linked to differences in glycosylation of a common polypeptide. *EMBO (Eur. Mol. Biol. Organ.) J.* 1:1239–1244.

Rouslahti, E., E. G. Hayman, and M. D. Pierschbacher. 1985. Extracellular matrices and cell adhesion. *Arteriosclerosis.* 5:581–594.

Staehelin, T., C. Stahli, D. S. Hobbs, and S. Pestka. 1981. A rapid quantitative assay of high sensitivity for human leukocyte interferon with monoclonal antibodies. *Methods Enzymol.* 79:589–595.

Streeter, P. R., E. L. Berg, B. N. Rouse, R. F. Bargatze, and E. C. Butcher. 1988a. A tissue-specific endothelial cell molecule involved in lymphocyte homing. *Nature (Lond.).* 331:41–46.

Streeter, P. R., B. T. N. Rouse, and E. C. Butcher. 1988b. Immunohistologic and functional characterization of a vascular addressin involved in lymphocyte homing into peripheral lymph nodes. *J. Cell Biol.* 107:1853–1862.

Stryer, L. 1978. Fluorescence energy transfer as a spectroscopic rules. *Annu. Rev. Biochem.* 47:819–846.

Titus, J. A., R. Haugland, S. O. Sharrow, and D. M. Segal. 1982. Texas red, a hydrophilic, red-emitting fluorophore for use with fluorescein in dual parameter flow microfluorometric and fluorescence microscopic studies. *J. Immunol. Methods.* 50:193–204.

Wu, N. W., S. Jalkanen, P. R. Streeter, and E. C. Butcher. 1988. Evolutionary conservation of tissue-specific lymphocyte–endothelial cell recognition mechanisms involved in lymphocyte homing. *J. Cell Biol.* 107:1845–1852.